Ab initio studies on the vibrational and thermal properties of Al_3Li

Zhiqiang Li and John S. Tse
Steacie Institute for Molecular Sciences, National Research Council of Canada, Ottawa, Ontario, Canada K1A 0R6
(Received 10 November 1999; revised manuscript received 27 January 2000)

A direct method is used to calculate phonon dispersions of Al_3Li based on the Hellmann-Feynman forces obtained from first-principles plane-wave pseudopotential calculations. The vibrational and thermodynamic properties of Al_3Li are calculated by using the quasiharmonic approximation at finite temperature, in comparison with the calculations of Al_4 in fcc structure to understand the alloying effect of Li. The calculated quantities, such as phonon dispersions, Grüneisen parameter, heat capacity, thermal expansion coefficient, and bulk modulus as a function of temperature, are discussed and compared with available experimental data.

I. INTRODUCTION

Electronic-structure calculations based on density-functional theory (DFT) in the local-density approximation (LDA) have proved to be effective tools for studying the zero-temperature energetics of many systems, ranging from bulk materials to surfaces, interfaces, and clusters.[1] With increasingly powerful computers and efficient algorithms, large systems can be handled, and problems in the material science are now feasible. However, the application of *ab initio* methods to the study of thermodynamic properties such as phase diagrams,[2] defect energetics, nucleation, and growth remains challenging, especially for metallic systems.

For crystals, the key problem to study the thermodynamics is to calculate the phonon contributions to the free energy. First-principles molecular-dynamics methods such as the Car-Parrinello method[3] can be used to determine thermal properties. However, since the ionic degrees of freedom are treated classically, these simulations are not valid at temperatures comparable to or lower than the Debye temperature. A more conventional approach based on lattice dynamics, i.e., the quasiharmonic approximation,[4] proves to be both accurate and computationally efficient at temperatures far away from melting point where anharmonic is significant. In this approximation, the crystal free energy is calculated by adding a dynamical contribution of free energy of harmonic oscillators corresponding to the crystal vibrational modes to the static contribution which is easily calculated by a standard DFT package. Anharmonic effects are included through the explicit volume dependence of the vibrational frequencies. The quasiharmonic approximations allows an explicit account of quantum effects on nuclear motion which can be important below the Debye temperature. Furthermore, analysis of the normal vibration modes and of their individual contribution to the free energy can reveal the mechanism driving the thermal expansion, phase transitions, and crystal instability. Calculations based on the various semiempirical methods[5,6] and *ab initio*[7–13] methods suggest that the quasiharmonic approximation provides a reasonable description of the thermodynamic properties of many bulk materials below the melting point.

Density-functional perturbation theory[14,15] (DFPT) is by now a common and well-established tool for calculating the vibrational properties from first principles. A very comprehensive review of phonon dispersion dispersion calculations has recently presented by Gonze.[15] Because of its complexity and being computationally demanding, the calculations of the full phonon spectrum as a function of volume are still a challenging problem for intermetallic alloys. We have developed a direct method[16] to calculate the phonon dispersions based on the Hellmann-Feynman forces obtained from DFT calculations on the supercell of a system with finite amplitude perturbation. The size of the supercell is determined by the range of the interatomic interactions, which could be quite large for systems showing phonon anomalies such as Nb and V. This method is much more efficient for complex systems with many atoms in the unit cell and could be easily extended to metallic systems, thanks to the recent developments of DFT algorithms which make it possible for the calculation of accurate total energy and force for several hundred to thousand atoms in the unit cell. Among other advantages, the direct method can produce the real-space interatomic force constants (IFC), which can be checked if the interactions diminish with the size of the supercell. Studies with similar methods have been reported on simple metals,[17,18] semiconductors,[8,19] and insulators,[16] and on transition metal rhodium.[20]

A few *ab initio* calculations of the thermodynamics of metallic systems have been published. Quong and Liu[10] reported DFPT calculations on the thermal expansion of several simple metals Al, Li, and Na by the quasiharmonic approximation. A similar study for silver has been presented by Xie *et al.*[12] van de Walle, Ceder, and Waghmare[11] calculated the vibrational entropy difference between ordered and disordered Ni_3Al. Recently, Slüiter, Weinert, and Kawazoe[21] published a first-principles calculation on the force constants of AlLi alloys.

In this paper, we apply the direct method to calculate the phonon dispersions and thermal properties of Al_3Li, such as the temperature dependence of thermal expansion coefficient, Grüneisen parameter, bulk modulus, and heat capacity, in comparison with the calculations for Al_4 in fcc structure. Al_4 and Al_3Li are selected for this study because (1) the interaction range is very short for both materials, (2) there exists a large collection of experimental thermodynamics data and theoretical calculations of phonon dispersions on Al,[22,23] which serves to calibrate the accuracy of the calculations, and (3) thermal lattice vibration affects significantly

the elastic constants and bulk modulus of Al_4 and Al_3Li,[24] which makes it difficult for a direct comparison between experiment and theory where temperature is usually neglected. For example, the bulk modulus of Al_3Li at room temperature is 66 GPa and 52 GPa at 523 K. (4) Al_3Li is a metastable phase precipitating in a solid solution matrix: it is very difficult to obtain reliable experimental results. An accurate first-principles study might serve as a valuable tool to supply the necessary information.

II. THEORETICAL METHODS

Calculations of total energy and Hellmann-Feynman forces are carried out by using VASP.[25] The VASP code applies the standard method in which the Kohn-Sham equations are solved self-consistently using a pseudopotential and plane-wave basis, based on the LDA. We have used norm-conserving pseudopotentials[26] for for Al and Li, which were generated with the atomic configuration of $3s^2 3p^1 3d^0$ and $2s^1 2p^0 3d^0$, and cutoff radius of 0.963 and 1.110 Å, respectively. The cutoff energy of 250 eV is used in the calculations. The summation over the Brillouin zone (BZ) is performed on a $6\times6\times6$ Monkhorst-Pack[27] k-point mesh, which results in 18 k points in the irreducible part of the Brillouin zone. The exchange-correlation functional of Perdew and Zunger[28] has been used in the calculations.

To calculate the phonon dispersions, we use both $2\times2\times2$ and $3\times3\times3$ supercells of fcc Al_4 and $L1_2$ Al_3Li, which contains 32 and 108 atoms, respectively, in order to check the convergence of IFCs. The Hellmann-Feynman forces are calculated for all atoms in the supercell with one atom displaced from the equilibrium position by about 0.5–1.0 % of the lattice constant. From the Hellmann-Feynman forces we can generate the IFCs by establishing the symmetry of the supercell: the interaction range is limited to the distance from the central atom of the supercell to the surface atom. The dynamical matrix is constructed to calculate the phonon frequencies. Details of obtaining force constants and phonon dispersions have been described in Ref. 16. We should point out that the direct method delivers correct phonon frequencies at these special wave vectors of the Brillouin zone, which are compatible with the supercell size. The symmetrization of the force constant matrix removes all third-order anharmonic effects.

With the force constants, the elastic constants can be calculated via the method of long waves, that is, the slopes of respective phonon dispersions at Γ.[20,21] The vibrational density of states (DOS) is obtained by an integration over the irreducible Brillouin zone with a Gaussian-broadened factor of 3.0 THz. By increase the q points in the BZ, one can improve the accuracy easily.

Within the quasiharmonic approximation, the free energy of a crystal is

$$F(T,V)=E(V)+\frac{1}{2}\sum_{\mathbf{q},n}\hbar\omega_n(\mathbf{q},V)+k_BT \times\sum_{\mathbf{q},n}\ln\left[1-\exp\left(-\frac{\hbar\omega_n(\mathbf{q},V)}{k_bT}\right)\right], \quad (2.1)$$

where $E(V)$ is the energy of a static lattice which is obtained from DFT total energy calculations, and $\omega_n(\mathbf{q},V)$ the phonon frequency of mode n and wave vector q for a given volume V. The linear thermal expansion coefficient $\alpha(T)$ is written as

$$\alpha(T)=\frac{1}{3B}\sum_{\mathbf{q},n}\gamma_n(\mathbf{q})c_{vn}(\mathbf{q},T), \quad (2.2)$$

where B is the isothermal bulk modulus, the $\gamma_n(\mathbf{q})$ th-mode Grüneisen parameter defined as

$$\gamma_n(\mathbf{q})=-\frac{d[\ln\omega_n(\mathbf{q},V)]}{d[\ln V]}, \quad (2.3)$$

and $c_{vn}(\mathbf{q},T)$ is the mode contribution to the specific heat defined as

$$c_{vn}(\mathbf{q},T)=\frac{\hbar\omega_n(\mathbf{q},V)}{V}\frac{d}{dT}\left[\exp\left(\frac{\hbar\omega_n(\mathbf{q},V)}{k_bT}\right)-1\right]^{-1}. \quad (2.4)$$

The total specific heat of the crystal will be the sum of all modes over the Brillouin zone:

$$C_v(T)=\sum_{\mathbf{q},n}c_{vn}(\mathbf{q},T). \quad (2.5)$$

The overall Grüneisen parameter is the weighted average of the mode Grüneisen parameters:

$$\gamma(T)=\frac{1}{C_v(T)}\sum_{\mathbf{q},n}\gamma_n(\mathbf{q})c_{vn}(\mathbf{q},T)=3B(T)\frac{\alpha(T)}{C_v(T)}. \quad (2.6)$$

The temperature dependence of the bulk modulus is obtained from

$$B(T)=V\left(\frac{\partial^2F(T,V)}{\partial V^2}\right)_T. \quad (2.7)$$

Due to anharmonicity, the heat capacity at constant pressure C_p is different from the heat capacity at constant volume C_v. The former, which is determined directly from experiments, is proportional to T at high temperature, while the latter converges to a constant which is given by the classical equipartition law: $C_v=3Nk_B$, where N is the number of atoms in the system. The relation between C_p and C_v is

$$C_p-C_v=\alpha^2(T)BVT. \quad (2.8)$$

III. RESULTS AND DISCUSSION

We first calculate the equilibrium lattice constant of fcc Al_4 and $L1_2$ Al_3Li by minimizing the total energy, and the results are given in Table I and the structure of Al_3Li is shown in Fig. 1. The calculated lattice constants in good agreement with experiments within 1%; the elastic constants are about 10% larger than the experimental values. The experimental values for Al are obtained at 175 K, (Ref. 22) and for Al_3Li at 294 K (Ref. 24). We will discuss the temperature effect on these quantities later, which leads to even better agreement with experiments.

TABLE I. Optimized lattice constants, elastic constants, and bulk modulus of Al and Al_3Li.

	Al_4		Al_3Li	
	Theory	Expt.[a]	Theory	Expt.[b]
a_0 (Å)	3.973	4.01	3.949	3.972
c_{11} (GPa)	106.1	107.0	120.0	123.6
c_{12} (GPa)	68.6	61.0	57.1	37.2
c_{44} (GPa)	33.6	28.0	70.4	66.0

[a]At 175 K, Ref. 22.
[b]At 294 K, Ref. 24.

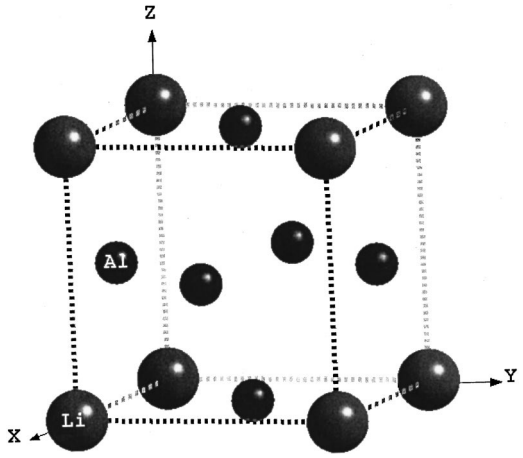

FIG. 1. Crystal structure of $L1_2$ Al_3Li alloy.

The IFCs extracted within $2\times2\times2$ and $3\times3\times3$ supercells have been examined. For Al, the $2\times2\times2$ supercell contains the atomic interactions of fifth nearest neighbors with 15 IFCs, while the $3\times3\times3$ supercell has the atomic interactions of ninth nearest neighbors with 32 IFCs. The IFCs beyond fifth nearest neighbor are about 1% of the second nearest neighbor IFCs and smaller than 5–10 % of the fifth nearest neighbor IFCs. Therefore, the atomic interaction of Al is very short ranged and actually the phonon dispersions calculated with $2\times2\times2$ supercells are almost exactly the same as those calculated with $3\times3\times3$ supercells. For Al_3Li, the atomic interaction is also short ranged, only three non-negligible IFCs, which are out of the range of $2\times2\times2$ supercell. We will use the results of $2\times2\times2$ supercells in the following discussions.

The calculated phonon dispersion curves for Al_4 and Al_3Li are shown in Figs. 2(a) and 2(b). By unfolding the phonon dispersions of fcc Al_4 to fcc Al, we find remarkable agreement with experiments, considering that we only used a $2\times2\times2$ supercell which has interactions up to the fifth nearest neighbor. The accuracy in this case is comparable to that of DFPT calculations. Unfortunately, to our best knowledge, there is no experimental phonon dispersion of Al_3Li available for a direct comparison. However, it is interesting to note that Al_3Li shows almost the same phonon dispersions as those of Ni_3Li obtained by inelastic neutron scattering.[31] For $2\times2\times2$ supercells, the calculated frequencies are exact (in the sense of a ''frozen phonon'') at the zone center (Γ) and boundaries (X,M,R). At other wave vectors, the accuracy of the phonon frequency depends on the interaction range of force constants.

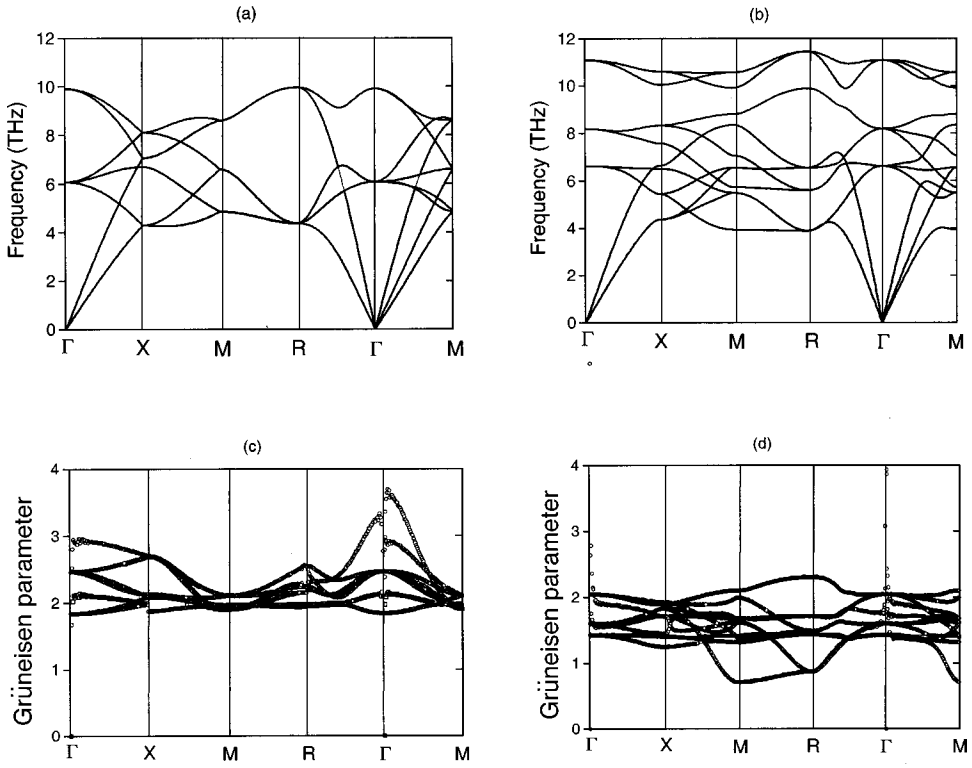

FIG. 2. Phonon dispersion of (a) fcc Al_4 and (b) Al_3Li and Grüneisen parameters of (c) fcc Al_4 and (d) Al_3Li along high-symmetry directions calculated at the equilibrium lattice constant.

TABLE II. Interatomic force constants (IFCs) of Al_3Li and Al_4 within the $2\times2\times2$ supercell, in units of N/m. Some symmetry-related IFCs are omitted for simplicity.

IFCs	Al_3Li	Al_4
Al-Al 0*XX*	−92.946	−79.778
Al-Al 0*XY*	−76.965	−79.778
Li-Li 0*XX*	−45.803	
Al-Al 1*XX*	10.710	10.661
Al-Al 1*XY*	−12.656	−11.499
Al-Al 1*YX*	−11.669	−11.499
Al-Al 1*ZZ*	−1.076	1.907
Al-Li 1*XX*	0.128	
Al-Li 1*XY*	6.418	
Al-Li 1*YY*	6.202	
Al-Al 2*XX*	3.427	2.232
Al-Al 2*YY*	0.098	−0.097
Li-Li 2*XX*	−0.144	
Li-Li 2*YY*	−0.039	
Al-Li 2*XX*	0.007	
Al-Li 2*YY*	0.614	
Al-Li 2*ZZ*	0.162	
Al-Al 3*XX*	−0.296	−0.406
Al-Al 3*XY*	−0.235	0.166
Al-Al 3*ZZ*	0.354	0.096
Al-Li 3*XX*	−0.262	
Al-Li 3*XY*	0.069	
Al-Li 3*YY*	0.458	
Al-Al 4*XX*	−0.059	0.106
Al-Al 4*YY*	0.145	0.106
Li-Li 4*XX*	−0.191	
Li-Li 4*YY*	−0.186	
Al-Al 5*XX*	0.015	0.186
Al-Al 5*YY*	0.015	0.186
Li-Li 5*XX*	0.024	
Li-Li 5*YY*	0.032	

Table II lists the IFCs of Al_3Li and Al_4 within $2\times2\times2$ spucells; on-site force constants are also included for discussion. Note that in the $L1_2$ structure, Al-Al interactions are not isotropic as that in fcc Al. For example, the *X* and *Y* directions are not equivalent for the Al atom in the *XY* plane; see Fig. 1. It is noted (1) most Al-Al interactions are enhanced in Al_3Li, especially for the on-site and the second nearest neighbor interactions. However, along *Y* direction, the on-site interaction is weaker, because there are no nearest Al-Al bonds in the *XZ* plane. (2) Al-Li and Li-Li interactions are weaker than those of Al-Al; therefore, Al_3Li shows anisotropic interatomic force constants. These are in agreement with the results of previous studies[29,30] that Al_3Li has a lower isotropic bulk modulus, higher Young's modulus, shear modulus and anisotropy constant. Figures 2(c) and 2(d) show the Grüneisen parameter of Al_4 and Al_3Li, respectively, as defined by Eq. (3), along some symmetry directions. The Grüneisen parameters are positive throughout the BZ for all branches. Al_4 has higher Grüneisen parameters than Al_4. At the Γ point of Al_4, some branches of transverse acoustic modes have a very high Grüneisen parameter, which is absent for the Grüneisen parameter of Al_3Li. This contributes to the increase of the overall Grüneisen parameter of Al at low temperature shown in Fig. 3, because at low temperature only the very-low-frequency phonons contribute to the summation in Eq. (2.3), while high-frequency phonons decay exponentially. The overall Grüneisen parameter of Al_4 is 2.14, which is higher than that of Al_3Li of 1.84; therefore, Al_4 has a larger thermal expansion coefficient than Al_3Li shown below. At low temperature, the overall Grüneisen parameters for Al_4 and Al_3Li show different behavior because of the different volume dependence of phonon frequencies around Γ point.

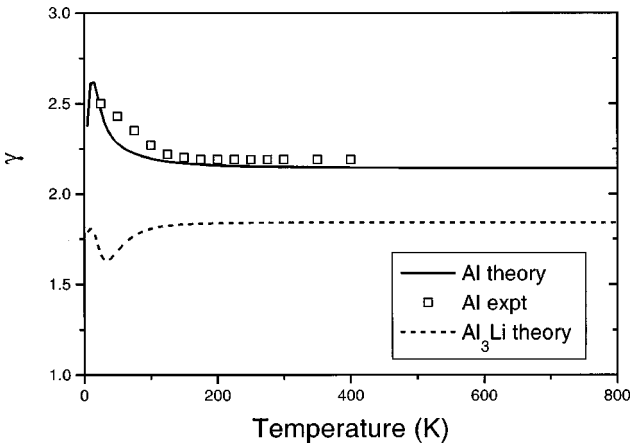

FIG. 3. Overall Grüneisen parameter of Al_4 and Al_3Li as a function of temperature. Experimental values for Al are from Ref. 22.

Figure 4 compares the DOS for fcc Al_4 and $L1_2$ Al_3Li. From Figs. 2 and 4, some interesting vibrational properties could be observed. The DOS of high-frequency modes in Al, about 8–10 THz, corresponding to the bond stretching between nearest Al atoms, is substantially reduced in Al_3Li because there are fewer nearest Al-Al bonds, while a narrow peak appears in the high-frequency end at about 10–12 THz, which is primarily due to the vibrations of light-mass Li sublattice. Nearest Li-Al vibrations also contribute to this high-frequency peak. From band-structure calculations,[29,30] a general trend is found that in AlLi alloys the Li atom donates its valence electron to strengthen the Al-Al bond, which re-

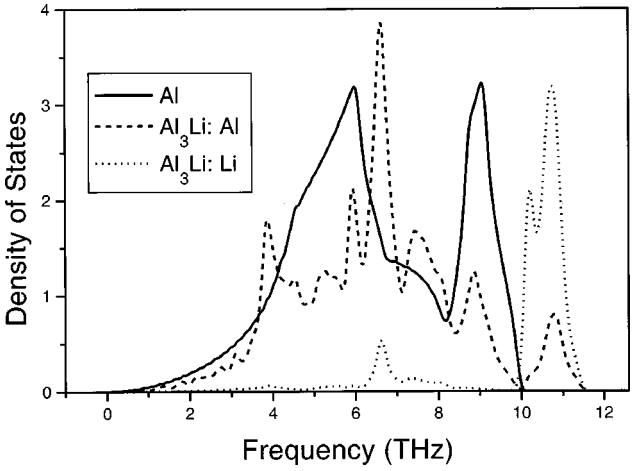

FIG. 4. Vibrational density of states for Al_4 and Al_3Li.

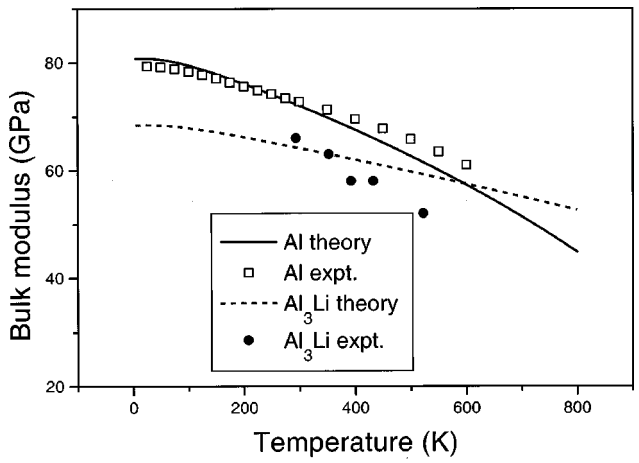

FIG. 5. Bulk modulus for Al_4 and Al_3Li as a function of temperature. Experimental values for Al are from Ref. 22, Al_3Li from Ref. 23.

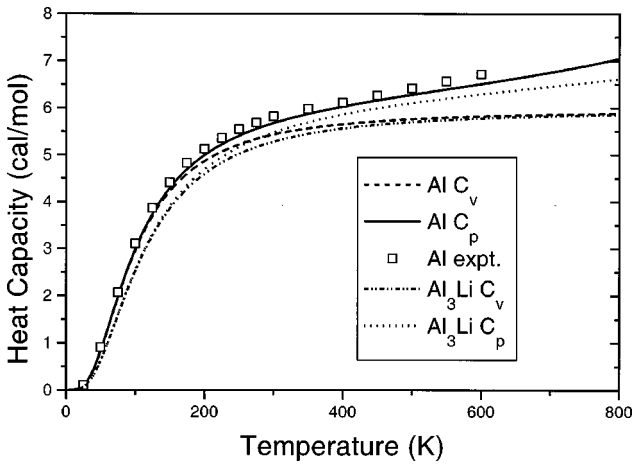

FIG. 7. Heat capacities at constant volume C_v and heat capacities at constant pressure C_p of Al_4 and Al_3Li as a function of temperature. Experimental values for Al are from Ref. 22.

sults in the narrow peak in the DOS at about 6.5 THz, which is mainly due to the Al sublattice optic modes. Moreover, the lattice constant of Al_3Li is shorter than that of fcc Al, and Li is lighter than Al. In general, the vibrational frequency moves higher when Al atoms are replaced by Li. Similar features have also been observed in the DOS of Ni_3Al.[31]

After the phonon frequencies at several volume $\omega_n(\mathbf{q},V)$ are obtained, it is straightforward to calculate the free energy $F(V,T)$ by Eq. (1) and then the bulk modulus $B(T)$ as a function of temperature; the results are shown in Fig. 5 along with the available experimental values. We find satisfactory agreement with experiments for Al. In the case of Al_3Li, the limited experimental value apparently decreases faster than our calculations. Because Al_3Li is a metastable phase precipitating in a solid solution matrix, it is very difficult to obtain reliable experimental results. It is noted from Fig. 5 that the bulk modulus of Al decreases more rapidly than that of Al_3Li and, over 600 K, Al_3Li even has a larger bulk modulus than Al. This could be rationalized since Al has more low-frequency modes than Al_3Li (see Fig. 4), which are easily activated even at low temperature, and hence makes the crystal softer.

The volume thermal expansion coefficient $\alpha(T)$ is obtained from Eq. (2) for Al and Al_3Li. Again, the experimental results are well reproduced for Al as shown in Fig. 6. Al_3Li has a lower thermal expansion coefficient than Al in the whole range of temperature, due to its smaller Grüneisen parameter; see Fig. 3.

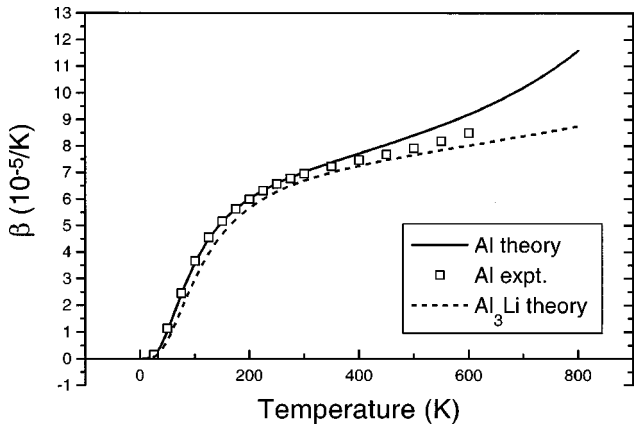

FIG. 6. Thermal expansion parameter of Al_4 and Al_3Li as a function of temperature. Experimental values for Al are from Ref. 22.

Finally, the specific heat capacities for Al_4 and Al_3Li are presented in Fig. 7. In the entire temperature range, the heat capacities of Al_4 are higher than those of Al_3Li below 500 K. From Fig. 4, it can be seen that the DOS of Al_4 is larger than that of Al_3Li below 10 THz (about 480 K). Over 600 K, the heat capacity at constant volume, C_v, approaches the classic limit, while the heat capacity at constant pressure increases monotonously with the temperature.

IV. CONCLUSION

In this paper, using the quasiharmonic approximation within density-functional theory, we have studied the thermal properties of $L1_2$ Al_3Li and made a comparison with fcc Al. Properties, such as phonon dispersions, the thermal expansion coefficient, Grüneisen parameters, bulk modulus, and heat capacity, have been obtained and compared with available experimental results. We demonstrated that the direct method can be applied to calculate the phonon dispersions of metals and metallic alloys with an accuracy comparable to density-functional perturbation theory calculations, on the condition that there be no anomaly in the phonon dispersions, which means the interaction range is small. By comparing the phonon dispersions of Al_4 and Al_3Li, we can rationalize the different thermodynamic properties of both materials and the effect of the Li atom. The Li atom was considered to donate its valent electron to enhance the Al-Al bonding Al_3Li alloys, which are manifested in its phonon dispersions and thermal properties.

ACKNOWLEDGMENTS

Z.Q.L. would like to thank Professor K. Parlinski and M. Slüiter for very helpful discussions on lattice dynamics theory and the NSERC/NRC for financial support.

[1] W. E. Pickett, Comput. Phys. Rep. **9**, 115 (1989).
[2] E. G. Moroni, G. Grimvall, and T. Jarlborg, Phys. Rev. Lett. **76**, 2758 (1996).
[3] R. Car and M. Parrinello, Phys. Rev. Lett. **55**, 2471 (1985).
[4] A. A. Maradudin, E. W. Montroll, E. H. Weiss, and I. P. Iaptova, *Theory of Lattice Dynamics in the Harmonic Approximation*, 2nd ed. (Academic, New York, 1971).
[5] C. H. Xu, C. Z. Wang, C. T. Chan, and K. M. Ho, Phys. Rev. B **43**, 5024 (1991).
[6] J. D. Althoff, D. Morgan, D. de Fontaine, M. Asta, S. M. Foiles, and D. D. Johnson, Phys. Rev. B **56**, R5705 (1997).
[7] P. Pavone, K. Karch, O. Schütt, W. Windl, D. Strauch, P. Giannozzi, and S. Baroni, Phys. Rev. B **48**, 3156 (1993); P. Pavone, S. Baroni, and S. de Gironcoli, *ibid.* **57**, 10 421 (1998).
[8] S. Wei, C. Li, and M. Y. Chou, Phys. Rev. B **50**, 14 587 (1994).
[9] G. M. Rignanese, J. P. Michenaud, and X. Gonze, Phys. Rev. B **53**, 4488 (1996).
[10] A. A. Quong and A. Y. Liu, Phys. Rev. B **56**, 7767 (1997).
[11] A. van de Walle, G. Ceder, and U. V. Waghmare, Phys. Rev. Lett. **80**, 4911 (1998).
[12] J. Xie, S. de Gironcoli, S. Baroni, and M. Scheffler, Phys. Rev. B **59**, 965 (1999).
[13] G. Kern, G. Kresse, and J. Hafner, Phys. Rev. B **59**, 8551 (1999).
[14] S. Baroni, P. Giannozzi, and A. Testa, Phys. Rev. Lett. **58**, 1861 (1987).
[15] X. Gonze, Phys. Rev. B **55**, 10 337 (1996); X. Gonze and Ch. Lee, *ibid.* **55**, 10 355 (1996).
[16] K. Parlinski, Z. Q. Li, and Y. Kawazoe, Phys. Rev. Lett. **78**, 4063 (1997); Phys. Rev. B **61**, 272 (2000).
[17] K. Kunc and R. M. Martin, Phys. Rev. Lett. **48**, 406 (1982).
[18] W. Frank, C. Elsasser, and M. Fahnle, Phys. Rev. Lett. **74**, 1791 (1995).
[19] G. Kresse, J. Furthmüller, and J. Hafner, Europhys. Lett. **32**, 729 (1995).
[20] A. Eichler, K. P. Bohnen, W. Reichardt, and J. Hafner, Phys. Rev. B **57**, 324 (1998).
[21] M. Slüiter, W. Weinert, and Y. Kawazoe, Phys. Rev. B **59**, 4100 (1999).
[22] D. C. Wallace, *Thermodynamics of Crystals* (Dover, New York, 1972).
[23] There are many calculations on the phonon dispersions of fcc Al. See, for example, the recent one of S. Gironcoli, Phys. Rev. B **51**, 6773 (1995) and Ref. 10.
[24] W. Müller, E. Bubeck, and V. Gerald, *Aluminium-Lithium Alloys III* (Institute of Metals, London, 1986), p. 435.
[25] G. Kresse and J. Furthmüller, Comput. Mater. Sci. **6**, 15 (1996); Phys. Rev. B **54**, 11 169 (1996).
[26] G. Kresse and J. Hafner, J. Phys.: Condens. Matter **6**, 8245 (1994).
[27] H. Monkhorst and J. Pack, Phys. Rev. B **13**, 5188 (1976).
[28] J. P. Perdew and A. Zunger, Phys. Rev. B **23**, 5048 (1981).
[29] X. Q. Guo, R. Podloucky, J. H. Xu, and A. J. Freeman, Phys. Rev. B **41**, 12 432 (1990); X. Q. Guo, R. Podloucky, and A. J. Freeman, J. Mater. Res. **6**, 324 (1991).
[30] M. J. Mehl, Phys. Rev. B **47**, 2948 (1993).
[31] C. Stassis, F. X. Kayser, C. K. Loong, and D. Arch, Phys. Rev. B **24**, 3048 (1981).